



LAWRENCE
LIVERMORE
NATIONAL
LABORATORY

UCRL-PROC-212117

Diode Pumped Alkali Vapor Lasers - A New Pathway to High Beam Quality at High Average Power

R. H. Page, C. D. Boley, A. M. Rubenchik, R. J.
Beach

May 10, 2005

Solid State and Diode Laser Technology Review
Los Angeles, CA, United States
June 7, 2005 through June 9, 2005

Disclaimer

This document was prepared as an account of work sponsored by an agency of the United States Government. Neither the United States Government nor the University of California nor any of their employees, makes any warranty, express or implied, or assumes any legal liability or responsibility for the accuracy, completeness, or usefulness of any information, apparatus, product, or process disclosed, or represents that its use would not infringe privately owned rights. Reference herein to any specific commercial product, process, or service by trade name, trademark, manufacturer, or otherwise, does not necessarily constitute or imply its endorsement, recommendation, or favoring by the United States Government or the University of California. The views and opinions of authors expressed herein do not necessarily state or reflect those of the United States Government or the University of California, and shall not be used for advertising or product endorsement purposes.

Diode Pumped Alkali Vapor Lasers—A New Pathway to High Beam Quality at High Average Power

R. H. Page, C. D. Boley, A. M. Rubenchik, and R. J. Beach

Lawrence Livermore National Laboratory
7000 East Ave.
Livermore CA 94551-0808

Resonance-transition alkali-vapor lasers have only recently been demonstrated [1,] but are already attracting considerable attention. Alkali-atom-vapor gain media are among the simplest possible systems known, so there is much laboratory data upon which to base performance predictions. Therefore, accurate modeling is possible, as shown by the zero-free-parameter fits [2] to experimental data on alkali-vapor lasers pumped with Ti:sapphire lasers. The practical advantages of two of the alkali systems—Rb and Cs—are enormous, since they are amenable to diode-pumping [3,4.] Even without circulating the gas mixture, these lasers can have adequate cooling built-in owing to the presence of He in their vapor cells. The high predicted (up to 70%) optical-to-optical efficiency of the alkali laser, the superb (potentially 70% or better) wall-plug efficiency of the diode pumps, and the ability to exhaust heat at high temperature (100C) combine to give a power-scalable architecture that is lightweight. A recent design exercise [5] at LLNL estimated that the system “weight-to-power ratio” figure of merit could be on the order of 7 kg/kW, an unprecedented value for a laser of the 100 kW class. Beam quality is expected to be excellent, owing to the small dn/dT value of the gain medium.

There is obviously a long way to go, to get from a small laser pumped with a Ti:sapphire or injection-seeded diode system (of near-perfect beam quality, and narrow linewidth) [1, 4] to a large system pumped with broadband, multimode diode-laser arrays. We have a vision for this technology-development program, and have already built diode-array-pumped Rb lasers at the 1 Watt level. A setup for demonstrating Diode-array-Pumped Alkali vapor Lasers (DPALs) is shown in Figure 1. In general, use of a highly-multimode, broadband pump source renders diode-array-based experiments much more difficult than the previous ones done with Ti:sapphire pumping. High-NA optics, short focal distances, and short vapor cells are needed.

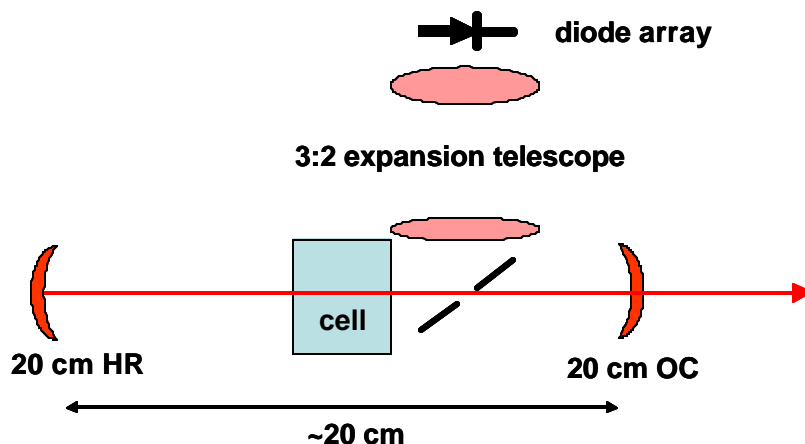


Figure 1. A multimode diode array pumps a thin (~2 mm) alkali-vapor cell via a “holey mirror” whose aperture allows traversal of the resonated beam. The nearly-confocal resonator’s mode fills a small portion of the pumped region, whose diameter is 0.6 mm.

The 20-W output of a 780 nm diode array is imaged via a telescope into the 2 mm gap of a refillable stainless-steel vapor cell whose interior windows are made of sapphire. A “holey mirror” allows the resonated beam to pass unimpeded (albeit at a penalty of ~10% of on-axis pump intensity.) Since the diode array’s NA was large (~0.2,) its depth of focus was lengthened by telescoping its image diameter up from 0.4 mm to 0.6 mm. The low-order spot of a near-confocal stable cavity overlaps the pumped region with about 28% efficiency. For these experiments, the He pressure was set at 2 atm and the ethane fill pressure was 90 Torr.

Peak DPAL output powers (cell at 190 C)

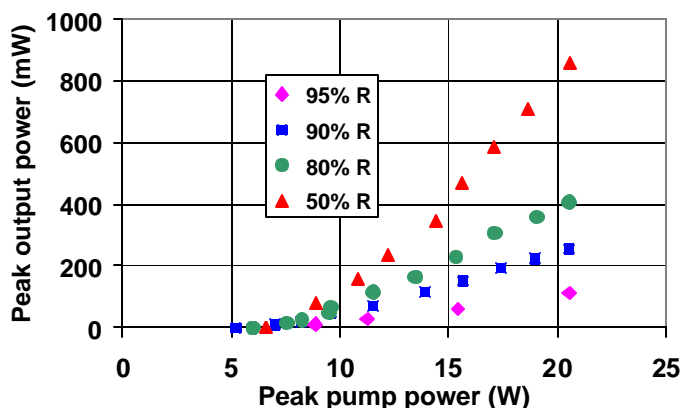


Figure 2. Slope plots of peak output power (5% duty cycle) vs output coupler reflectivity, with the cell held at 190 C. This starting value of cell temperature was above optimum. The 50% output coupler gave the highest output power.

It was desired to “scope out” the DPAL characteristics in order to find its optimum performance, and to provide data for comparing against predictions of our laser-modeling code. Two convenient variables are the output coupling (modified by changing cavity mirrors,) and the cell temperature. Figure 2 displays “slope plots” of output vs input power for each of 4 output couplers ranging in nominal reflectivity from 95% down to 50%. These data were obtained with the pump diodes operating at 5% duty cycle (100 Hz, 500 μ sec.) As a starting point, the cell was set at 190 C. Increasing the output coupling did not increase the pump threshold dramatically; this is evidence of high intracavity loss.

Peak output vs cell temperature (50% OC)

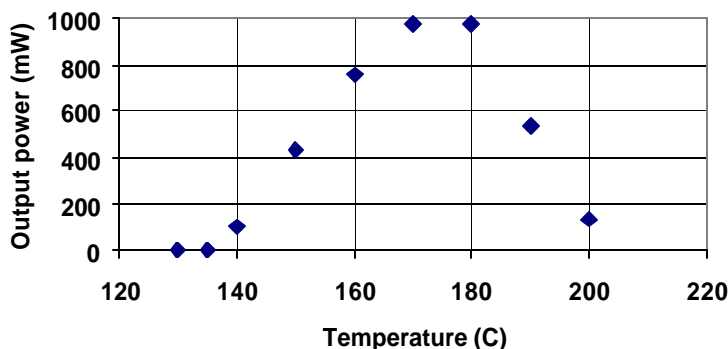


Figure 3. Output power vs. cell temperature, using the 50% output coupler. The apparent optimum is evidently 170 – 180 C, although gradual degradation in cell transmittance skews the peak toward lower temperatures. (Note the sag in the 190 C point, with respect to the 190 C slope plots.)

When the temperature was scanned up (Fig. 3) after the output-coupler exchanges, it was found that the highest laser output (very nearly 1.0 Watt) was obtained at 170 – 180 C, a bit lower than expected. The obtainable output power at 190 C was not as high as it had been—there was a decline from 854 mW to 536 mW. So, we conclude that the laser performance was degrading as time passed, and the optimum may well be above 180 C. Measurements of the lasing threshold (also something we can predict and model) vs temperature are shown in Fig. 4.

Threshold drive vs temperature (50% OC)

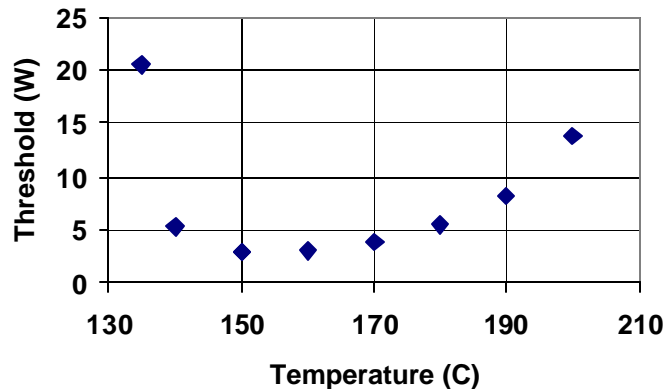


Figure 4. Pump threshold vs cell temperature. The broad minimum at 150 – 170 C corresponds to several tens of nepers (e-foldings) of small-signal absorption on the D_2 transition. Because of bleaching, minimum threshold and maximum output power do not occur simultaneously as the cell temperature is varied.

Naturally, there is high interest in power-scaling the DPALs to serve in various defensive capacities. A conceptual tens-of-kW design (taken from [2]) is shown in Fig. 5; it is based around an unstable resonator and a “hollow lens duct” for delivering pump light. Even larger output powers can be envisaged with similar architectures without flowing the gas fill.

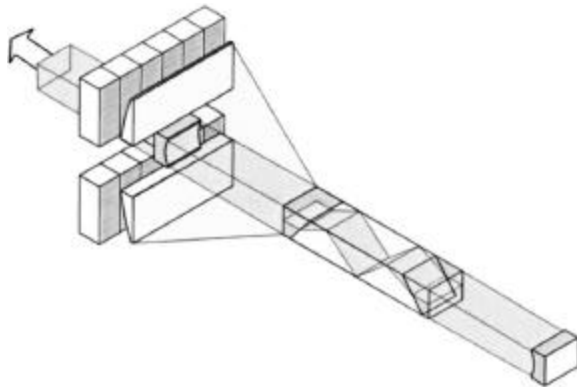


Figure 5. Unstable-resonator DPAL of length ~1 m and 20 – 30 kW nominal output power. Its operating temperature is ~100 C, facilitating removal of waste heat from the top and bottom surfaces. Its static gas fill (mostly He) is ~25 atm. Zig-zag operation is achieved with prism-shaped windows on the vapor cell.

For illuminating remote targets, a good beam from a single aperture is generally desired. The projected high efficiency and concomitant low cooling requirement for a 100 kW DPAL system suggest [5] an overall package mass below 1000 kg, enabling deployment in many scenarios not realistic for less-efficient lasers (including the best solid-state lasers known.)

Because the DPALs operate at wavelengths somewhat unfamiliar in the directed-energy community, it is appropriate to examine the propagation and lethality characteristics. The atmospheric transmission (Fig. 6(a)) appears good for the Cs DPAL at 895. Most of the

attenuation at that wavelength is due to aerosol scatter. A more subtle concern is the combined effect of diffraction and turbulence—one might expect that although the theoretical beam divergence could be less, beam breakup would be more severe at shorter wavelengths. We have modeled the far-field spot size at a moving target (mortar round a few km distant,) as a function of time, as shown in Fig. 6(b). To simulate turbulence, the refractive-index structure-function value [6] was set to $C_n^2 = 10^{-14} \text{ m}^{-2/3}$ at 10 m height (and assumed to vary inversely with height.) It is seen that of the three wavelengths chosen, 895 nm gives the smallest spot.

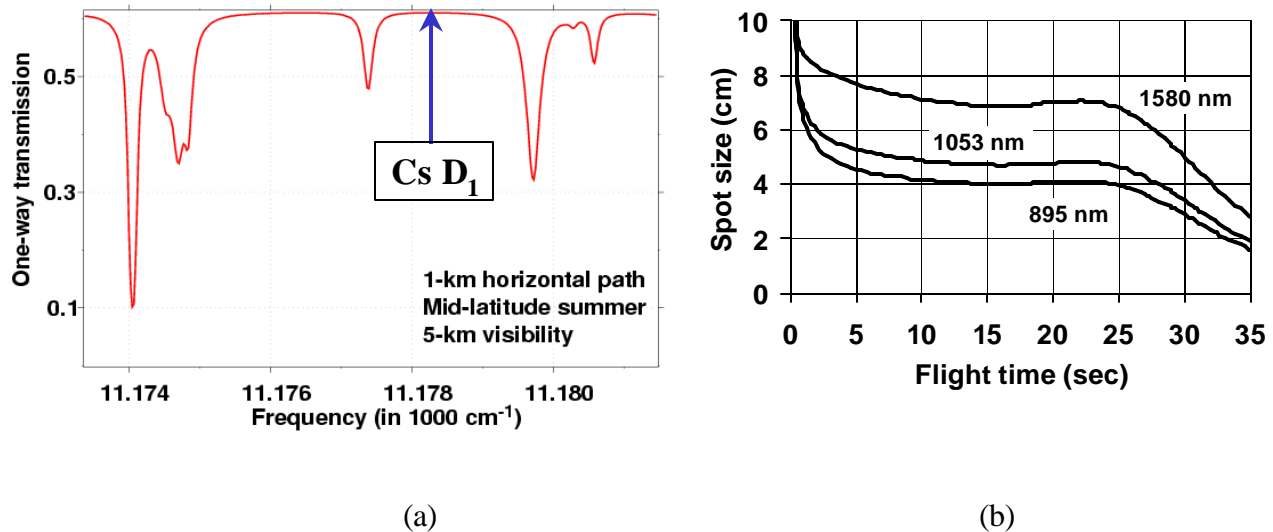


Figure 6(a). HITRAN atmospheric-transmission spectrum near the 11178.3 cm^{-1} Cs laser line, which appears to be well displaced from absorption resonances. (b) Time-dependent spot sizes for laser beams of three different wavelengths irradiating a mortar round, launched toward an asset from a distance of 3.5 km. The laser is situated 1 km from the asset, at cross-range. The spot size is determined by diffraction and atmospheric turbulence. The turbulence profile is a frequently-used one corresponding to 45-degree propagation. The 895 nm beam produces the smallest spot (and couples best to the target), making it the most lethal. 895 nm is evidently an excellent wavelength to aim at a remote target.

It is well to hit a target with a well-placed, compact beam, but also important for the light to be absorbed. Data on absorptances for common metals—iron and aluminum—from standard sources [7, 8] are listed in Table I for four different laser wavelengths near the Cs DPAL.

Table I. Iron and Aluminum Absorptances for Different Laser Wavelengths

Laser	Wavelength (μm)	Absorptance (Fe)	Absorptance (Al)
Cs DPAL	0.895	0.51	0.11
Nd:glass	1.053	0.48	0.06
I	1.315	0.46	0.04
O ₂ “air laser”	1.58	0.36	0.03

Both of these metals absorb best at the Cs DPAL D₁ line 895 nm wavelength. So, considering the expected propagation and absorption characteristics, a high-power Cs DPAL would be a strong candidate in a directed-energy scenario.

Power beaming is another example of a directed-energy application in which a DPAL could be quite useful. Unfortunately, space constraints do not allow for discussion of the relative merits concerning photovoltaic response, propagation into space, etc. Suffice it to say that, pending demonstration of a high-power system, additional options for power-beaming light sources will eventually exist.

Acknowledgement

This work was supported by the U. S. Department of Energy under contract W-7405-ENG-48 at UC LLNL and the High Energy Laser Joint Technology Office (HEL JTO.)

References

- [1] W.F. Krupke, R.J. Beach, V.K. Kanz, and S.A. Payne, "Resonance transition 795-nm rubidium laser," *Optics Lett.* **28**, 2336 - 2338 (2003.)
- [2] R.J. Beach, W.F. Krupke, V.K. Kanz, S.A. Payne, M. A. Dubinskii, and L. D. Merkle, "End-pumped CW alkali vapor lasers: Experiment, model and power scaling," *J. Opt. Soc. Am. B* **21**, 2151 - 2163 (2004.)
- [3] Ralph H. Page, Raymond J. Beach, V. Keith Kanz, and William F. Krupke, "First demonstration of a diode-pumped gas (alkali vapor) laser," CLEO 2005 abstract CMAA1.
- [4] T. Ehrenreich, B. Zhdanov, T. Takekoshi, S. P. Phipps, and R. Knize, "Diode pumped caesium laser," *Electronics Lett.* **41**, 20058388 (2005.)
- [5] R. Yamamoto et al, LLNL; private communication (2005.)
- [6] R. K. Tyson, Principles of Adaptive Optics (Academic Press, New York, 1991,) pp 31 – 36.
- [7] Y. S. Touloukian and D. P. DeWitt, eds., Thermophysical Properties of Matter, vol. 7: Thermal Radiative Properties—Metallic Elements and Alloys (IFI/Plenum, New York, 1970)
- [8] Edward D. Palik, ed., Handbook of Optical Constants in Solids, *Academic Press* (1985)